Published in final edited form as:
Bioorg Med Chem Lett. 2010 January 1; 20(1): 392. doi:10.1016/j.bmcl.2009.10.061.

Bioisosterism of Urea-Based GCPII Inhibitors: Synthesis and Structure-Activity Relationships Studies

Haofan Wang[a,#], **Youngjoo Byun**[a,#], **Cyril Barinka**[b], **Mrudula Pullambhatla**[a], **Hyoeun C. Bhang**[c], **James J. Fox**[a], **Jacek Lubkowski**[b], **Ronnie C. Mease**[a], and **Martin G. Pomper**[a,c,*]

[a]Department of Radiology, Johns Hopkins Medical Institutions, Baltimore, MD 21231, USA

[c]Department of Pharmacology and Molecular Sciences, Johns Hopkins Medical Institutions, Baltimore, MD 21231, USA

[b]Center for Cancer Research, National Cancer Institute at Frederick, Frederick, MD 21702

Abstract

We report a strategy based on bioisosterism to improve the physicochemical properties of existing hydrophilic, urea-based GCPII inhibitors. Comprehensive structure-activity relationship studies of the P1' site of ZJ-43- and DCIBzL-based compounds identified several glutamate-free inhibitors with K_i values below 20 nM. Among them, compound **32d** (K_i = 11 nM) exhibited selective uptake in GCPII-expressing tumors by SPECT-CT imaging in mice. A novel conformational change of amino acids in the S1' pharmacophore pocket was observed in the X-ray crystal structure of GCPII complexed with **32d**.

Keywords

PSMA; glutamate carboxypeptidase II; molecular imaging; radiopharmaceutical; SPECT

Glutamate carboxypeptidase II (GCPII) is a type II zinc-dependent metalloprotease that cleaves *N*-acetylaspartylglutamate (NAAG) to release *N*-acetylaspartate (NAA) and glutamate (Glu) in the brain.[1, 2] Excessive production and release of Glu in the synaptic cleft may over-stimulate glutamate receptors, leading to Glu-associated neurotoxicity and neuronal death. A glutamatergic imbalance has been proposed in the pathophysiology of a variety of neurological diseases including ischemia, traumatic brain injury, neuropathic pain, amyotrophic lateral sclerosis, diabetic polyneuropathy, and schizophrenia.[3–8] Accordingly, maintaining Glu homeostasis at the synapse is a goal in the prevention and treatment of neuropsychiatric disease. Among the enzymes that modulate such Glu concentrations, GCPII is a potential target for effecting beneficial intrasynaptic Glu concentrations.

GCPII has also been identified in non-neuronal tissues including kidney, small intestine, and prostate. Consequently GCPII has also been referred to as the prostate-specific membrane

*Corresponding Author: Martin G. Pomper, M.D., Ph.D., Johns Hopkins Medical Institutions, 1550 Orleans Street, 492 CRB II, Baltimore, MD 21231, Tel: 410-955-2789 (T), Fax: 443-817-0990 (F), mpomper@jhmi.edu.
[#]These authors contributed equally.

antigen (PSMA) in the prostate and as folate hydrolase (FOLH1) in the intestine. PSMA is over-expressed on the surface of androgen-independent prostate cancer cells and its active site is located in the extracellular region. Cell-surface expression and up-regulation in prostate tumors render PSMA an attractive target for the diagnosis and possibly therapy of prostate cancer.[9,] 10 The FOLH1 activity of GCPII hydrolyzes γ-linked glutamates from poly-γ-glutamyl folate to produce folic acid, which can then be uptaken by folate receptors in the intestine.11 GCPII has also been identified in neovasculature of most solid tumors.12 That vascular expression enhances GCPII as a cancer imaging and therapeutic target.

Previously, we have synthesized a number of urea-based GCPII inhibitors radiolabeled with ^{99m}Tc, ^{125}I, ^{18}F and ^{11}C, which demonstrated strong GCPII inhibitory potency *in vitro* and selective uptake in PSMA-expressing tumors *in vivo* in single photon emission computed tomography (SPECT) and positron emission tomography (PET) small animal imaging studies.[13–17] Recent crystallographic studies of complexes between GCPII and low molecular weight ligands, including our urea-based inhibitors, elucidated their binding modes within the active site of GCPII, revealing that the S1 pocket of GCPII is more tolerant toward structural modification than glutamate-binding, S1' (pharmacophore) pocket.[18–24] Consequently, we have taken advantage of the structural freedom provided by the S1 pocket for the development of imaging probes for prostate cancer.

In parallel with our effort to develop PSMA-based imaging agents for prostate cancer, we have attempted to develop imaging agents for Glu-associated neurological disease. Using *in vitro* autoradiography we previously determined GCPII levels in rodent brain by measuring specific binding of [^{125}I]DCIT (Figure 1), a potent GCPII inhibitor.[24] By employing GCPII knockout mice, we showed that [^{125}I]DCIT demonstrated binding to rodent brain in a GCPII gene-dose dependent fashion. Using a similar technique we reported that GCPII levels in prefrontal cortex and temporal lobe in postmortem samples of patients with schizophrenia were significantly lower than age-matched controls.[25] Another tricarboxylic acid with the urea core, ZJ-43 (Figure 1), exhibited strong *in vitro* GCPII inhibition (K_i = 0.8 nM) with cloned human GCPII and demonstrated analgesic activity in inflammatory and neuropathic pain models.[26] However, high doses of ZJ-43 (50–100 mg/kg) needed to be administered in order to demonstrate an analgesic effect, due to low penetration of the blood-brain barrier (BBB). DCIBzL (Figure 1), the most potent urea-based GCPII inhibitor (K_i = 0.01 nM) that we have synthesized to date, showed high and prolonged tumor uptake as well as high target to nontarget tissue ratios in *ex vivo* biodistribution studies.[14] Based on these findings with existing urea-based GCPII inhibitors, we designed novel urea-based GCPII inhibitors with increased lipophilicity through two approaches: 1) bioisosterism of the P1' glutamate using two potent GCPII inhibitors ZJ-43 and DCIBzL as templates, and 2) prodrugs of DCIT, which is beyond the scope of this paper. Here we discuss the synthesis, structure-activity relationships (SAR), X-ray crystal structures and *in vivo* SPECT-CT imaging studies of new urea-based GCPII inhibitors designed for greater penetration of the BBB. The aim of this study was to identify novel scaffolds to replace Glu in the P1' site in order to improve BBB penetration by passive diffusion while retaining GCPII-binding affinity needed for detection by imaging. The current work focused on replacing one of the three carboxylic acids in ZJ-43 and DCIBzL with more lipophilic functional groups.

Ever since urea-based dipeptides with high GCPII binding affinity were reported by Kozikowski and co-workers in 2000, a number of urea-based GCPII inhibitors as therapeutic or imaging agents have been synthesized and evaluated.[27–29] Two potent urea-based PSMA inhibitors, ZJ-43 and DCIBzL (Figure 1), were selected as templates for substituting Glu in the P1' site with bioisosteric functional groups. Compounds ZJ-43 and DCIBzL demonstrated potent *in vitro* GCPII inhibitory activities (K_i = 0.8 nM and 0.01 nM) but have low ClogD values (−6.1 and − 5.16), too hydrophilic for the penetration of the BBB by passive diffusion.

Recent site-directed mutagenesis experiments of amino acids in the vicinity of the GCPII active site revealed that mutation of the amino acids that contact the γ-carboxylate of the P1' glutamate had less effect on enzymatic activity compared to mutation of those that contact the α-carboxylate in the P1 and P1'site.[18] Therefore, we focused on modifications of the γ-carboxylate group of the P1' site in ZJ-43 and DCIBzL in this study.

We replaced the side chain of the P1' glutamate moiety in ZJ-43 with a variety of more lipophilic bioisosteres including phenylglycine (Class A, Scheme 1), tyrosine (Class B, Scheme 1) and others (Class C, Scheme 1). The designed bioisosteric analogs of ZJ-43 were prepared by following a synthetic route outlined in Scheme 1. Briefly, treatment of Leu-methyl ester with triphosgene and triethylamine in dichloromethane generated an isocynate intermediate, which was subsequently reacted with amino acids in free or methyl ester form in DMF to yield the urea analogs. Hydrolysis of the methyl ester with LiOH in H_2O/CH_3CN afforded the corresponding diacids (**2–5, 14, 15, 17 19**) in 20–55% yield. For the synthesis of the isopropyl ester series (**7, 9**), we utilized the same synthetic strategy as the methyl ester analogs shown in Scheme 1. The detailed synthetic procedures and analytical data for each compound among ZJ-43 analogs (**1–22**) are available in supporting information. In cases where non-natural amino acids were not commercially available, they were synthesized according to Scheme 2. Reaction of substituted benzaldehydes with ammonia in methanol (7N) in the presence of trimethylsilyl cyanide afforded aminonitrile analogs (**23–26**) in 40–65% yield. The aminonitriles were hydrolyzed in aqueous hydrochloric acid (6 N) under reflux to give a racemic mixture of amino acids (**27–30**) in 70–80% yield. Racemic amino acids were directly coupled with the reactive isocyanate intermediate in Scheme 1. All final compounds (**1–22**) were purified by high-performance liquid chromatography (HPLC) and their chemical structures were confirmed by NMR and ESI-MS. *In vitro* GCPII inhibitory activities were determined using a fluorescence-based NAALADase assay.[14] As summarized in Scheme 1, K_i values of twenty-two ZJ-43 analogs were higher than 80 nM. Although the absolute K_i values of ZJ-43 bioisosteres fell short of criteria for *in vivo* imaging studies (K_i values of approximately ≤ 20 nM), which was estimated from the fact that the concentration of GCPII is ~ 40 fmol/mg protein in rodent brain[30] and that external imaging can be observed at least a 2:1 target:nontarget binding[31, 32], we could establish a relationship between *in vitro* GCPII inhibitory activities and different substituents at the phenyl ring of the phenylglycine analog. Briefly, introduction of a hydroxyl group at the 4-position (**3**) led to an increase in GCPII inhibitory potency relative to substitution at the 3-position (**1**) or at 3,5-positions (**4**), indicating that 4-OH is preferred in this series. However, the replacement of 4-OH with 4-F resulted in a significant decrease in GCPII potency. Preference for a functional group at the 3-position along with 4-OH is as follows: OCH_3 (**6**) > I (**8**), Br (**10**) > F (**12**), suggesting that a bulky substituent at the 3-position slightly increased the binding affinity. Vanillin analog **7** (M.W= 396.4, K_i = 81 nM, ClogD= −1.4), which has a hydroxyl group at the 4-position, a methoxy group at the 3-position and an isopropyl ester of leucine at the P1 site, was the most potent among the evaluated analogs. All compounds in the tyrosine (**14–18**), methionine (**19–20**), glutamine (**21**), and tryptophan (**22**) series were less active than **7**. However, because none of the ZJ-43 analogs showed an inhibitory activity lower than our initial ≤ 20 nM cut-off, we did not undertake *in vivo* studies with ZJ-43 analogs.

To increase GCPII inhibitory potency of our bioisoteres, we synthesized analogs of DCIBzL (K_i = 0.01 nM), one of the most potent GCPII urea-based inhibitors synthesized to date.[14] The crystal structure of GCPII complexed with DCIBzL (PDB ID: 3D7H) showed a peculiar binding pattern in the vicinity of the S1-pocket.[18] The iodophenyl group of DCIBzL projects into the arginine-patch region and resides in the accessory pocket delineated by side chains of arginines 463, 534 and 536 (Figure 3). The utilization of that sub-pocket increases DCIBzL potency by more than 80-fold compared to ZJ-43. We hypothesized that the iodophenyl-

substituted lysine moiety in place of the leucine of ZJ-43 would increase the binding affinity for GCPII.

To confirm the importance of the γ- and α-carboxylic acid groups at the P1' site, we replaced the P1' glutamic acid with glycine (**32a**) and γ-aminobutyric acid (**32b**), respectively. Both substitutions resulted in a dramatic decrease of GCPII inhibitory activity, indicating that both the α- and γ-carboxylates are important for GCPII binding although the glycine analog (**32a**, 1.32 μM) is slightly more potent than the GABA analog (**32b**, 3.43 μM). However, cyclopropanylglycine analog (**32c**, 318 nM) showed 4-fold stronger binding affinity for GCPII than **32a**, implying that a substituent at the α-carbon of the glycine may increase the binding potency. Encouraged by that result, we focused on the modification on the P1' side chain of DCIBzL (bearing the γ-carboxylic functionality) using substituted glycines. The synthesis of DCIBzL analogs is shown in Scheme 3. Briefly, N^{ε}-Boc-$_{L}$-lysine t-butyl ester was reacted with triphosgene and triethylamine in dichloromethane, followed by the addition of unnatural amino acid, to afford compounds in 30–70% yield. Protecting groups (t-butyl and t-Boc) were removed by the treatment with TFA. The terminal amine of Lys was coupled with *N*-succinimidyl-4-iodobenzoate to give compounds **32a–32t** (Scheme 3) in 50–75% yield.

Table 1 summarizes the K_i values and ClogD values of DCIBzL analogs. Introduction of hydrocarbon groups, which are more flexible and bulky than cyclopropane, resulted in a substantial increase in GCPII inhibitory activity. In particular, unsaturated hydrocarbon groups such as allylic (**32d**, 11 nM) and propagylic (**32e**, 5.3 nM) increased potency of GCPII inhibitory activity more significantly than the corresponding saturated analog (**32f**, 52.3 nM). However, analogs with heteroatom-containing functional groups including epoxide (**32g**), nitrile (**32h**) and amide (**32i**) were less active, with K_i values over 100 nM. Nevertheless, K_i values of sulfur-containing analogs (**32j** and **32k**) were 23 nM and 24 nM, respectively. Phenylglycine analogs **32l** (85 nM) and **32m** (285 nM) were not as potent as **32j** and **32k**.

To investigate the effects of stereochemistry on GCPII binding, compounds **32n–q** were synthesized. Maintenance of natural stereochemistry at the α-carbon is critical for GCPII inhibitory activity. Compounds **32n** (5.3 nM) and **32o** (16.2 nM), which have ($_{L}$)-configuration at the α-carbon, are much more potent than the corresponding ($_{D}$)-analogs **32p** (794 nM) and **32q** (795 nM). Thiazole-substituted **32r** (16.1 nM) displayed strong potency, similar to the thiophene-containing **32o**. However, compounds **32s** (105 nM) and **32t** (97 nM), substituted with a pyridine function, exhibited weaker inhibitory potency than the 5-membered heteroaromatic analogs (**32n**, **32o** and **32r**). Compound **32d** was further studied *in vivo* because it demonstrated a K_i value of 11 nM, which is below the cut-off value (K_i < 20 nM) for visualization by external imaging.[31, 32] Compound [^{125}I]**32d** was prepared as in Scheme 4. Precursor **31d** was reacted with *N*-succinimidyl-4-[^{125}I]iodobenzoate(S-[^{125}I]IB)[33] to afford [^{125}I]**32d** in 60% radiochemical yield. The specific radioactivity of [^{125}I]**32d** was 55.5 GBq/μmol. Mice bearing both PSMA-positive PIP and PSMA-negative Flu tumors were injected intravenously with 1.2 mCi of [^{125}I]**32d** *via* the lateral tail vein. SPECT-CT scanning of the brain of the mouse was performed immediately after the injection and on the whole body at 30 min and 120 min after injection. As seen in Figure 2, [^{125}I]**32d** exhibited selective uptake in the PSMA-positive PIP tumor over PSMA-negative Flu tumor at both time points. However, we did not observe any brain uptake of [^{125}I]**32d** (ClogD = −2.48) in the SPECT-CT imaging study, as expected, because it is still too hydrophilic to cross the BBB despite improved physicochemical properties compared to DCIBzL (ClogD = −5.16).

To elucidate the binding mode of **32d** in the active site of GCPII, we determined the X-ray crystal structure of GCPII in complex with **32d** (PDB ID: 3IWW). As shown in Figure 3, **32d** (represented in green) is positioned in the GCPII binding cavity in a manner similar to DCIBzL.[18] The 4-iodobenzoyl moiety resides inside the pocket accessory to the S1 site and

participates in π-cationic interactions with the guanidinium groups of Arg534 and Arg463. The urea carbonyl group interacts with the hydroxyl group of the Tyr552 and both P1 and P1' α-carboxylates are engaged primarily by the guanidinium groups of Arg534 and Arg536 (P1) and Arg210 (P1'), respectively. The allylic moiety spatially overlaps with the side chain of the P1' glutamate in DCIBzL, but the absence of interactions between the P1' side chain of **32d** and the Lys699 and Asn257 (as observed in the case of P1' glutamate) reduces somewhat its GCPII-inhibitory potency. Nevertheless, the allyl side chain contributes to the potency of **32d**, primarily *via* non-polar interactions with the side chains of Phe209, Leu261, and Leu428. This contribution is clearly documented by 120-fold tighter binding compared to compound **32a**, which is missing the P1' side chain altogether. Interestingly, an association with **32d** is accompanied by structural rearrangements at the bottom of the GCPII-S1' pocket, including displacement of the Lys699 side chain and a repositioning of the Leu259-Gly263 segment (Figure 3). Such variability has not been observed in any published GCPII structure and indicates additional spatial freedom of the S1' pocket that could be used for inhibitor design.

In summary, the SAR studies of ZJ-43 and DCIBzL analogs described herein have identified new scaffolds to replace the glutamic acid in the P1' region. These include the allyl, alkynl, furanyl, and thiophenyl moieties. Among them, compound **32d**, containing the allylic moiety, exhibited selective uptake in PSMA-positive tumors in SPECT-CT imaging studies. The GCPII crystal structure with **32d** showed a binding pattern similar to DCIBzL in the active site, along with a unique conformational change in the S1' pocket. However, compound **32d** is still too hydrophilic for brain imaging, suggesting that further structural modification is warranted.

Supplementary Material

Refer to Web version on PubMed Central for supplementary material.

Abbreviations

PSMA	prostate-specific membrane antigen
GCPII	glutamate carboxypeptidase II
NAAG	*N*-acetylaspartyl glutamate
NAALADase	*N*-acetylated-α-linked acidic dipeptidase
DCIT	(S)-2-(3-((S)-1-carboxy-2-(4-hydroxy-3-iodophenyl)ethyl)ureido) pentanedioic acid
DCIBzL	(*S*)-2-(3-((*S*)-1-carboxy-(4-iodobenzamido)pentyl)ureido)pentanedioic acid
ZJ-43	(S)-2-(3-((S)-1-carboxy-3-methylbutyl)ureido)pentanedioic acid
SPECT	single-photon emission computed tomography
SAR	structure-activity relationship.

Acknowledgments

The authors are grateful for financial support from the National Institutes of Health Grants MH080580 and CA092871 to M. G. P. The use of the Advanced Photon Source was supported by the U. S. Department of Energy (W-31-109-Eng38). J.L and C.B. acknowledge financial support from the National Cancer Institute, Center for Cancer Research.

References and notes

1. Robinson MB, Blakely RD, Couto R, Coyle JT. J. Biol. Chem 1987;262:14498. [PubMed: 3667587]

2. Byun, Y.; Mease, RC.; Lupold, SE.; Pomper Martin, G. Drug design of zinc-enzyme inhibitors. Supuran, CT.; Winum, J-Y., editors. New Jersey: John Wiley & Sons, Inc; 2009. p. 881-910.
3. Olszewski RT, Bukhari N, Zhou J, Kozikowski AP, Wroblewski JT, Shamimi-Noori S, Wroblewska B, Bzdega T, Vicini S, Barton FB, Neale JH. J. Neurochem 2004;89:876. [PubMed: 15140187]
4. Bacich DJ, Wozniak KM, Lu XCM, O'Keefe DS, Callizot N, Heston WDW, Slusher BS. J. Neurochem 2005;95:314. [PubMed: 16190866]
5. Neale JH, Olszewski RT, Gehl LM, Wroblewska B, Bzdega T. Trends Pharmacol. Sci 2005;26:477. [PubMed: 16055199]
6. Ghadge GD, Slusher BS, Bodner A, Dal Canto M, Wozniak K, Thomas AG, Rojas C, Tsukamoto T, Majer P, Miller RJ, Monti AL, Roos RP. Proc. Natl. Acad. Sci. U. S. A 2003;100:9554. [PubMed: 12876198]
7. Slusher BS, Vornov J, Thomas AG, Hurn PD, Harukuni I, Bhardwaj A, Traystman RJ, Robinson MB, Britton P, Lu XCM, Tortella FC, Wozniak SKM, Yudkoff M, Potier BM, Jackson PF. Nat. Med. (N. Y.) 1999;5:1396.
8. Zhou J, Neale JH, Pomper MG, Kozikowski AP. Nat. Rev. Drug Discovery 2005;4:1015.
9. Bostwick DG, Pacelli A, Blute M, Roche P, Murphy GP. Cancer 1998;82:2256. [PubMed: 9610707]
10. Israeli RS, Powell CT, Fair WR, Heston WDW. Cancer Res 1993;53:227. [PubMed: 8417812]
11. Pinto JT, Suffoletto BP, Berzin TM, Qiao CH, Lin S, Tong WP, May F, Mukherjee B, Heston WDW. Clin. Cancer Res 1996;2:1445. [PubMed: 9816319]
12. Liu H, Moy P, Kim S, Xia Y, Rajasekaran A, Navarro V, Knudsen B, Bander NH. Cancer Res 1997;57:3629. [PubMed: 9288760]
13. Banerjee SR, Foss CA, Castanares M, Mease RC, Byun Y, Fox JJ, Hilton J, Lupold SE, Kozikowski AP, Pomper MG. J. Med. Chem 2008;51:4504. [PubMed: 18637669]
14. Chen Y, Foss CA, Byun Y, Nimmagadda S, Pullambhatla M, Fox JJ, Castanares M, Lupold SE, Babich JW, Mease RC, Pomper MG. J. Med. Chem 2008;51:7933. [PubMed: 19053825]
15. Foss CA, Mease RC, Fan H, Wang Y, Ravert HT, Dannals RF, Olszewski RT, Heston WD, Kozikowski AP, Pomper MG. Clin. Cancer Res 2005;11:4022. [PubMed: 15930336]
16. Mease RC, Dusich CL, Foss CA, Ravert HT, Dannals RF, Seidel J, Prideaux A, Fox JJ, Sgouros G, Kozikowski AP, Pomper MG. Clin. Cancer Res 2008;14:3036. [PubMed: 18483369]
17. Pomper MG, Musachio JL, Zhang J, Scheffel U, Zhou Y, Hilton J, Maini A, Dannals RF, Wong DF, Kozikowski AP. Mol. Imaging 2002;1:96. [PubMed: 12920850]
18. Barinka C, Byun Y, Dusich CL, Banerjee SR, Chen Y, Castanares M, Kozikowski AP, Mease RC, Pomper MG, Lubkowski J. J. Med. Chem 2008;51:7737. [PubMed: 19053759]
19. Barinka C, Hlouchova K, Rovenska M, Majer P, Dauter M, Hin N, Ko Y-S, Tsukamoto T, Slusher BS, Konvalinka J, Lubkowski J. J. Mol. Biol 2008;376:1438. [PubMed: 18234225]
20. Barinka C, Rovenska M, Mlcochova P, Hlouchova K, Plechanovova A, Majer P, Tsukamoto T, Slusher BS, Konvalinka J, Lubkowski J. J. Med. Chem 2007;50:3267. [PubMed: 17567119]
21. Barinka C, Starkova J, Konvalinka J, Lubkowski J. Acta Crystallogr., Sect. F: Struct. Biol. Cryst. Commun 2007;F63:150.
22. Klusak V, Barinka C, Plechanovova A, Mlcochova P, Konvalinka J, Rulisek L, Lubkowski J. Biochemistry 2009;48:4126. [PubMed: 19301871]
23. Mesters JR, Barinka C, Li W, Tsukamoto T, Majer P, Slusher BS, Konvalinka J, Hilgenfeld R. Embo J 2006;25:1375. [PubMed: 16467855]
24. Davis MI, Bennett MJ, Thomas LM, Bjorkman PJ. Proc. Natl. Acad. Sci. U. S. A 2005;102:5981. [PubMed: 15837926]
25. Guilarte Tomas R, Hammoud Dima A, McGlothan Jennifer L, Caffo Brian S, Foss Catherine A, Kozikowski Alan P, Pomper Martin G. Schizophr. Res 2008;99:324. [PubMed: 18191545]
26. Yamamoto T, Hirasawa S, Wroblewska B, Grajkowska E, Zhou J, Kozikowski A, Wroblewski J, Neale Joseph H. Eur. J. Neurosci 2004;20:483. [PubMed: 15233757]
27. Kozikowski AP, Nan F, Conti P, Zhang J, Ramadan E, Bzdega T, Wroblewska B, Neale JH, Pshenichkin S, Wroblewski JT. J. Med. Chem 2001;44:298. [PubMed: 11462970]
28. Kozikowski AP, Zhang J, Nan F, Petukhov PA, Grajkowska E, Wroblewski JT, Yamamoto T, Bzdega T, Wroblewska B, Neale JH. J. Med. Chem 2004;47:1729. [PubMed: 15027864]

29. Nan F, Bzdega T, Pshenichkin S, Wroblewski JT, Wroblewska B, Neale JH, Kozikowski AP. J. Med. Chem 2000;43:772. [PubMed: 10715144]

30. Guilarte TR, McGlothan JL, Foss CA, Zhou J, Heston WD, Kozikowski AP, Pomper MG. Neurosci. Lett 2005;387:141. [PubMed: 16006038]

31. Eckelman WC, Reba RC, Gibson RE, Rzeszotarski WJ, Vieras F, Mazaitis JK, Francis B. J. Nucl. Med 1979;20:350. [PubMed: 43884]

32. Eckelman WC, Reba RC, Kelloff GJ. Drug Discovery Today 2008;13:748. [PubMed: 18617011]

33. Wilbur DS, Hadley SW, Hylarides MD, Abrams PG, Beaumier PA, Morgan AC, Reno JM, Fritzberg AR. J. Nucl. Med 1989;30:216. [PubMed: 2738650]

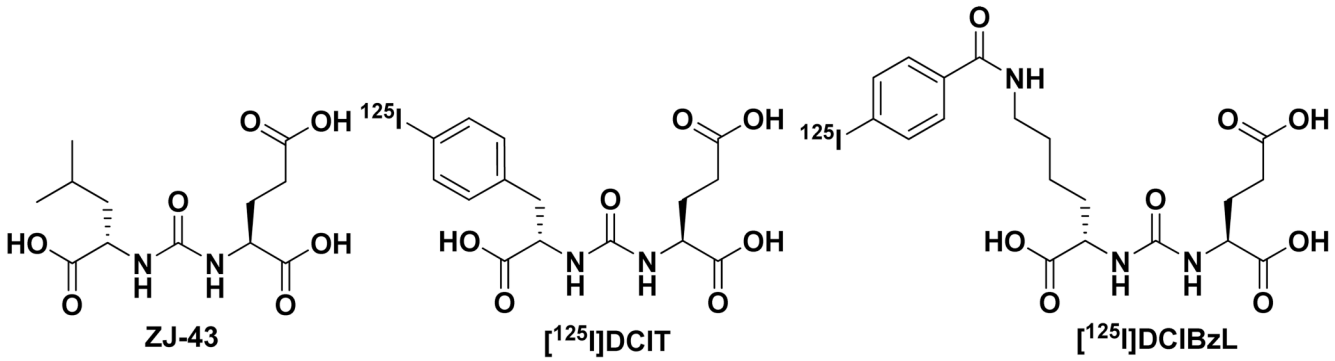

Figure 1.
Chemical structures of ZJ-43, [^{125}I]DCIT and [^{125}I]DCIBzL

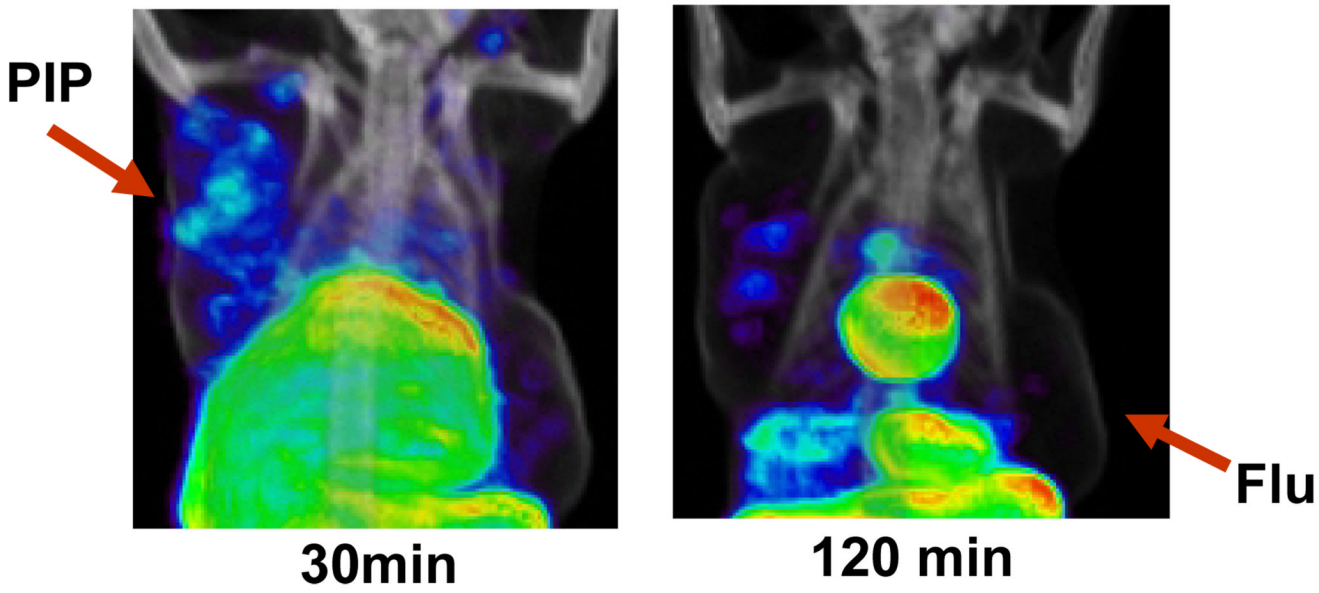

Figure 2.
SPECT-CT images of **32d** at 30 min and 120 min after injection

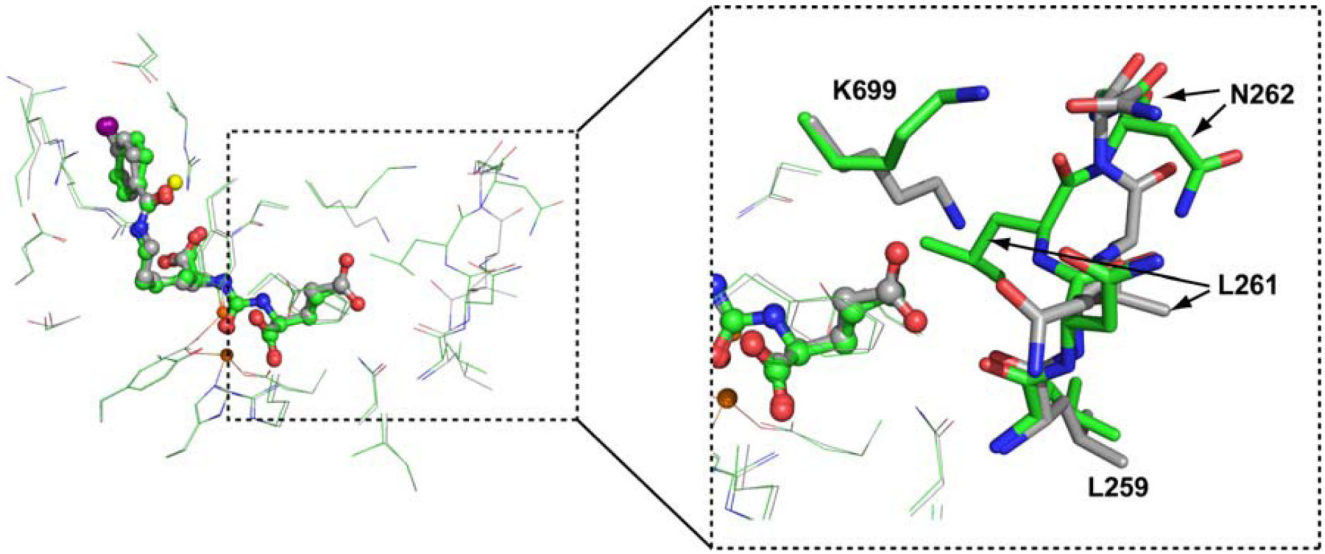

Figure 3.
Crystal structure of **32d** (ball and stick in green) with GCPII overlaid with DCIBzL. Amino acids in the S1' site were shown in stick type.

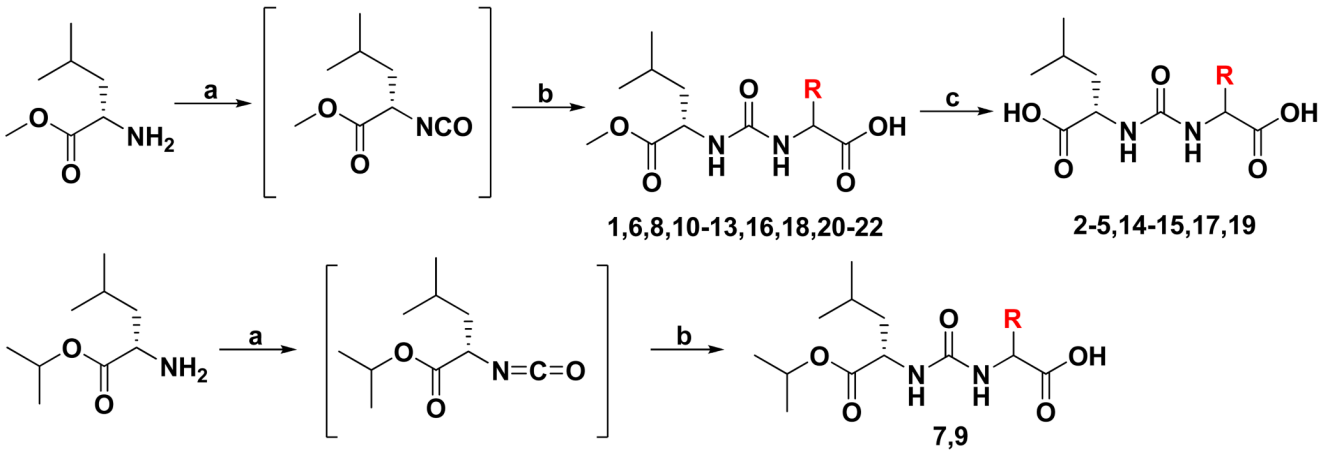

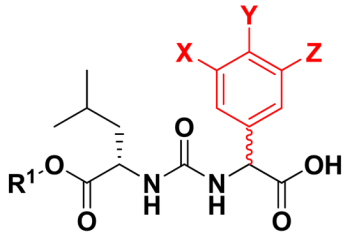

A

1 (> 1 mM): X=OH, Y=H, Z=H, R^1=CH_3
2 (> 1 mM): X=OH, Y=H, Z=H, R^1=H
3 (775 nM): X=H, Y=OH, Z=H, R^1=H
4 (13 uM): X=OH, Y=H, Z=OH, R^1=H
5 (250 nM): X=OCH_3, Y=OH, Z=H, R^1=H
6 (153 nM): X=OCH_3, Y=OH, Z=H, R^1=CH_3
7 (81 nM): X=OCH_3, Y=OH, Z=H, R^1=$CH(CH_3)_2$
8 (475 nM): X=I, Y=OH, Z=H, R^1=CH_3
9 (275 nM): X=I, Y=OH, Z=H, R^1=$CH(CH_3)_2$
10 (400 nM): X=Br, Y=OH, Z=H, R^1=CH_3
11 (575 nM): X=Br, Y=OH, Z=Br, R^1=CH_3
12 (3 uM): X=F, Y=OH, Z=H, R^1=CH_3
13 (> 1 mM): X=OCH_3, Y=F, Z=H, R^1=CH_3

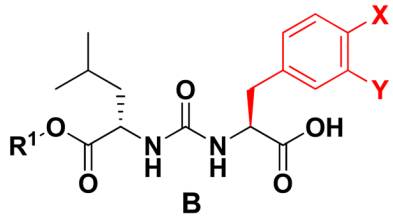

B

14 (700 nM): X=OH, Y=H R^1=H
15 (13 uM): X=OH, Y=I, R^1=H
16 (> 1 mM): X=H, Y=OH, R^1=CH_3
17 (3 uM): X=H, Y=COOH, R^1=H
18 (> 1 mM): X=H, Y=COOH, R^1=CH_3

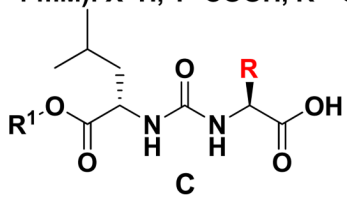

C

19 (3.5 uM): R^1=H, R=$CH_2CH_2SCH_3$
20 (> 1 mM): R^1=CH_3, R=$CH_2CH_2SCH_3$
21 (7.5 uM): R^1=CH_3, R=$CH_2CH_2CONH_2$
22 (> 1 mM): R^1=CH_3, R=CH_2-Indolyl (3-)

Scheme 1.

Synthetic route for ZJ-43 analogs and their K_i values

Reagents: a) triphosgene, TEA/CH_2Cl_2, b) appropriate unnatural amino acids, TEA, DMF, c) LiOH, H_2O/CH_3CN

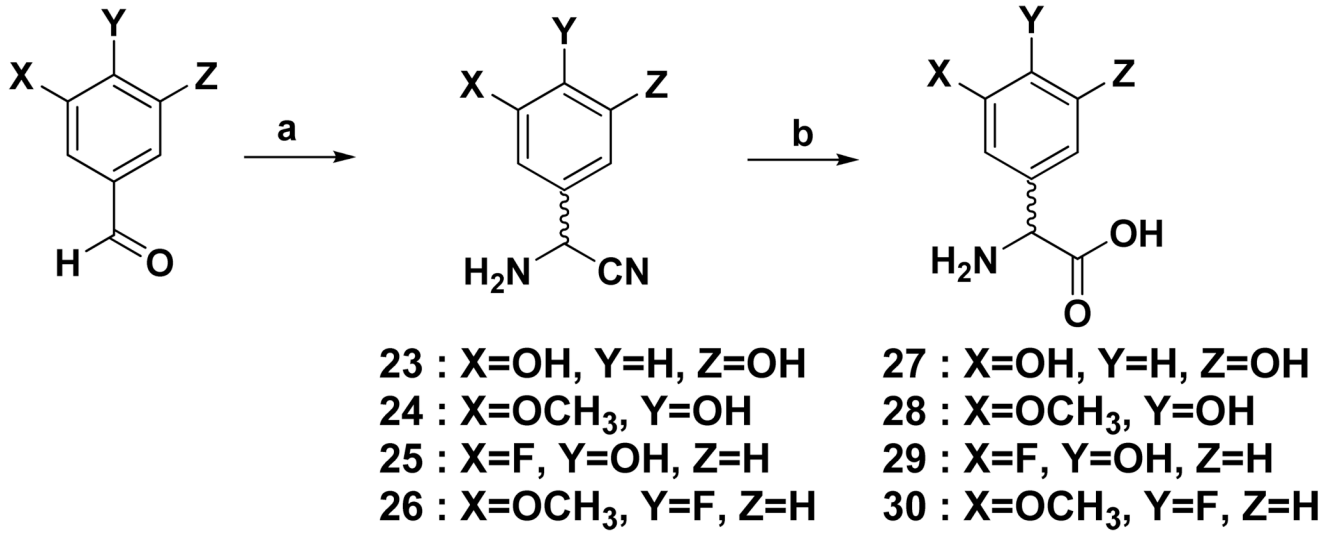

Scheme 2.
Synthetic route for non-commercial amino acids
Reagents: a) TMSCN, NH_3/MeOH, b) 6N-HCl

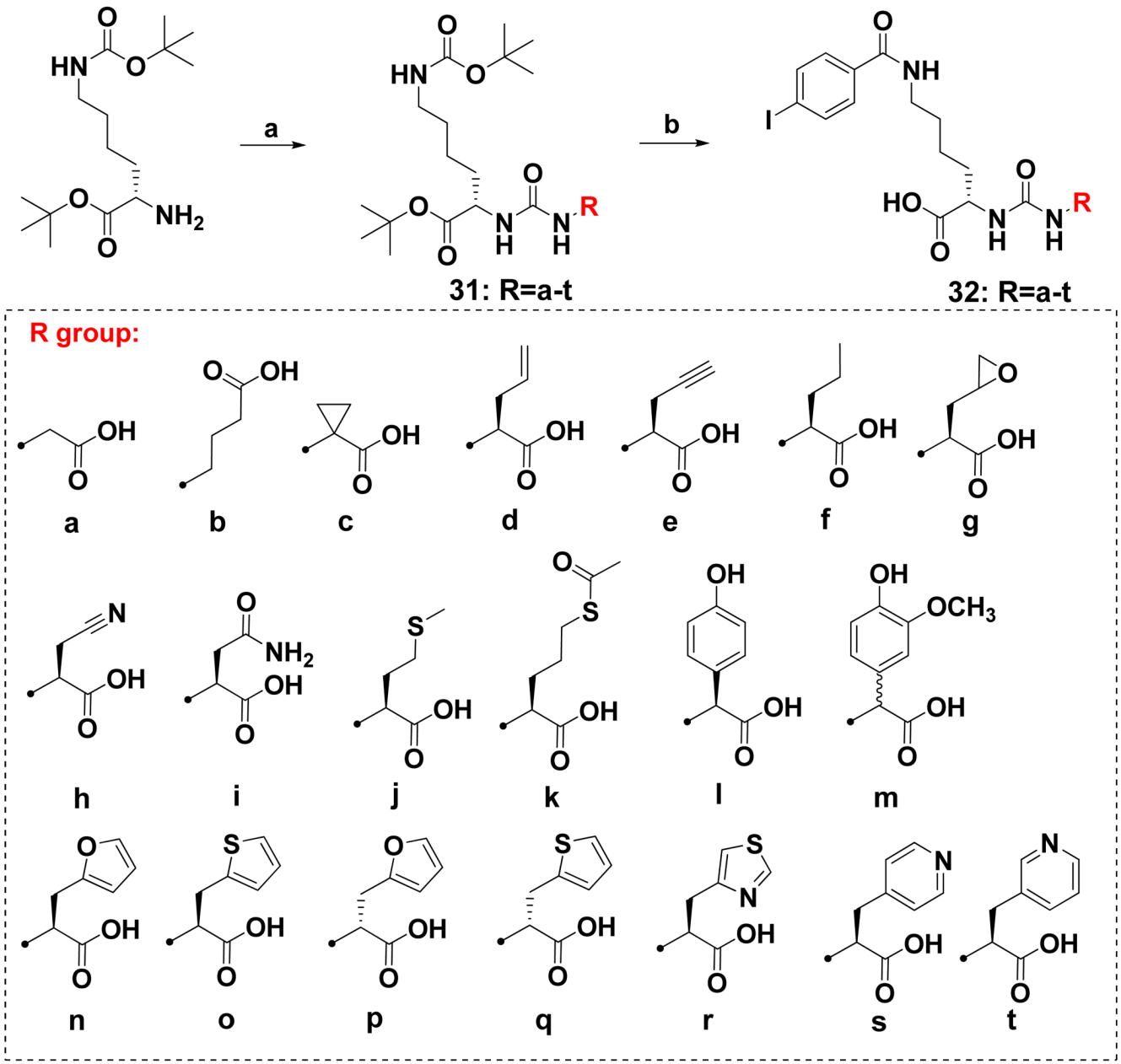

Scheme 3.

Synthetic route for DCIBzL analogs

Reagents: a) i: triphosgene, TEA/CH_2Cl_2, ii: appropriate unnatural amino acids, TEA, b) i: TFA, ii: N-succinimidyl-4-iodobenzoate, TEA/DMF

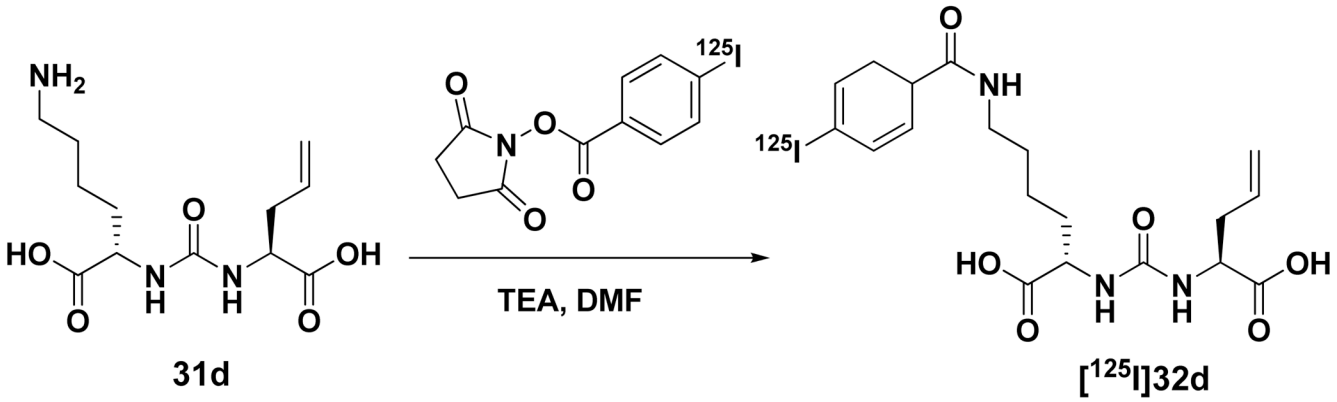

Scheme 4.
Synthetic route for [^{125}I]**32d**

Table 1

Summary of K_i, CI and CLogD values of DCIBzL analogs.

Compds	K_i (nM)[a]	CI (95%, nM)[b]	CLogD[c]
32a	1320	692–2510	−3.76
32b	3430	820–7520	−3.35
32c	318	107–946	−3.92
32d	11.0	8.2–14.8	−2.48
32e	5.3	3.8–7.5	−2.77
32f	52.3	32.3–84.7	−2.35
32g	254	187–345	−2.89
32h	132	83–211	−3.46
32i	320	206–497	−4.25
32j	23.0	12.0–44.0	−2.37
32k	24.1	15.6–37.3	−2.31
32l	85.1	63.7–114	−2.51
32m	285	181–452	−2.81
32n	5.3	3.8–7.4	−2.40
32o	16.2	11.7–22.6	−1.88
32p	794	266–2370	−2.40
32q	795	535–1130	−1.88
32r	16.1	11.3–23.0	−3.34
32s	105	65–170	−2.80
32t	97.2	54–175	−2.96
ZJ-43	0.75	0.60–0.94	−6.13
DCIBzL	0.01[14]		−5.16

[a] Values are means of at least three experiments.

[b] 95% confidence interval.

[c] Values are calculated by ACD ABS9.0